Journal of Rock Mechanics and Tunnelling Technology (JRMTT)
30 (1) 2024 pp 39-56

Available online at www.isrmtt.com

Assessment of GIS-based Landslide Susceptibility Using Bivariate and Multivariate Approach - A Case Study of Kashmir Himalayas

Iftikhar Hussain Beigh, Syed Kaiser Bukhari*

Department of Civil Engineering NIT Srinagar, J&K, India

**Email: iftikharbeigh@nitsri.ac.in*

ABSTRACT

National Highway -1 (NH-1) in Kashmir joins the union territories of J&K and Ladakh covering mainly Baramulla, Srinagar, and Kargil cities. The route passes through high mountain ranges and most of the roads cling to mountain sides. The NH-1 is considered to be one of the lifelines of the region, which is affected adversely by recurring occurrence of natural hazards such as landslides, earthquakes, cloudburst, avalanche etc. In the present work, the 45km road stretch along NH-1, Kashmir Himalaya was chosen for the landslide susceptibility zonation (LSZ) mapping using frequency ratio (FR) and analytical hierarchy process (AHP) models in GIS environment. The landslide inventory map was prepared from the visual interpretation of satellite images, field survey data, and other secondary data. The landslide locations were randomly divided into two groups: Training samples and validation samples. There are 10 landslide causative parameters that were considered for the analyses. LSZ maps were generated by calculating the relationship between the landslide influencing factors with training landslide data in the case of the FR model but for the AHP model, pair-wise comparisons were made to derive the weights and final score. The LSZ maps were prepared using FR and AHP models and classified into five different susceptibility zones. The LSZ maps were compared and validated with the validation landslide dataset using the Area Under Curve (AUC) method. The AUC value of the FR model is 0.803 showing better prediction accuracy than the AHP model (AUC value is 0.789). As a result, the FR method was found to be a reliable and effective method for assessing landslide-susceptible areas. Moreover, planners, developers, and engineers in the region could find the study's findings useful for slope management, land-use planning, and landslide mitigation measures.

Keywords: Landslide susceptibility; National Highway-1 (NH-1); FR; AHP; Kashmir Himalayas

1. INTRODUCTION

Landslides are the most common and recurring natural hazard in the Kashmir Himalaya due to its unique geological and topographic environment. Landslides have a negative impact on the region's socioeconomics by inflicting significant loss of human life and infrastructure. However, high-resolution remote sensing and field data are required for mapping landslides as points or polygons. Besides, a landslide Inventory mapping of small dimensions can be well represented by a point on a 1:50,000 scale map or much lower scales. The three essential components of a landslide study are landslide susceptibility, landslide hazard, and landslide risk. Landslide susceptibility mapping, also known as zonation, is the subdivision of

topography into zones with varying likelihoods of landslide occurrence. It covers the landslide deposit's spatial distribution, size, position, and displacement (Varnes 1984; Guzzetti et al., 1999; Fell et al., 2008). In this study, two approaches: Bivariate (Frequency Ratio Model) and multicriteria evaluation (AHP) were used to assess the landslide susceptibility along the Baramulla-Uri Road of NH-1. The findings of this study can aid in the identification of landslide-prone areas in the study area. Moreover, the study will be highly beneficial for construction planners, environmental engineers, and risk managers to plan and mitigate landslide hazards in the studied region.

The study area falls in Survey of India's topographic no's 43J/4, 43J/8, and 43F/16, covering a total area of 479.81 km^2. The study was conducted on a 45km road section of NH-1 between latitudes 34°1'35.38"N and 34°15'20.942"N and longitudes 73°57'41.4"E and 74°24'10.11" E. (Fig.1). The region spans in altitude from 1098 to 3475m above mean sea level. It has a rugged and uneven topography. Most of the route follows the south banks of the Jhelum River downstream of Baramulla town. Along the route, the towns of Baramulla, Khanpora, Sheeri, Gantamulla, Mahura, Lagama, and Uri are well-known destinations. On the southern side of the route is a spectacular view of the mighty Pir Panjal range, which reaches an average elevation of 1,400 to 4,100m above mean sea level (MSL). On the southwest side of the Pir Panjal Range there are several thrust faults in southeast directions including the MCT/Panjal, MBT/Murree, and BF subsidiary faults (Thakur et al., 2010). The geomorphology of the studied area is dominated by heavily dissected hills and valleys whereas the soil is dominated by coarse loamy type. The study area has a humid sub-tropical type of climate, with cold, wet winters and cool, dry summers. From December to May, the region receives the most snowfall and from June to September, the least. The road segment experiences slope failures because of mild erosion, strong precipitation, tectonic activity, and other anthropogenic activities such as road widening, building construction, etc.

Figure 1 - Location map of the study area

2. COLLECTION OF DATA AND METHODOLOGY

2.1 Geospatial Database Creation

High-resolution sentinel imageries were combined with Google Earth imageries, followed by extensive fieldwork to locate landslides along the NH-1 and its surroundings. For landslide susceptibility mapping along the Baramulla-Uri Road of NH-1 Road in the Kashmir Himalaya, ten contributing variables were considered, including slope gradient, elevation, slope aspect, slope curvature, proximity to road, proximity to drainage, proximity to lineament, geology, land use and land cover, and rainfall. The drainage map was extracted from dem, and lineaments were driven from the NRSC Bhuwan site. The geological map was motivated by the Geological map of Jammu and Kashmir. The LULC was derived from Landsat 8 OLI/TIRS using supervised classification and the maximum likelihood approach. The Indian Metrological Department (IMD) gridded datasets for the past 30 years (1991-2021) were used to prepare rainfall maps. To produce the reliability of the landslide inventory, past literature, govt official data, global data archives, and high-resolution imageries followed by detailed field checkups (2019–2021) were conducted. The steps in generating a landslide susceptibility map are sequential and outlined in Figure 2.

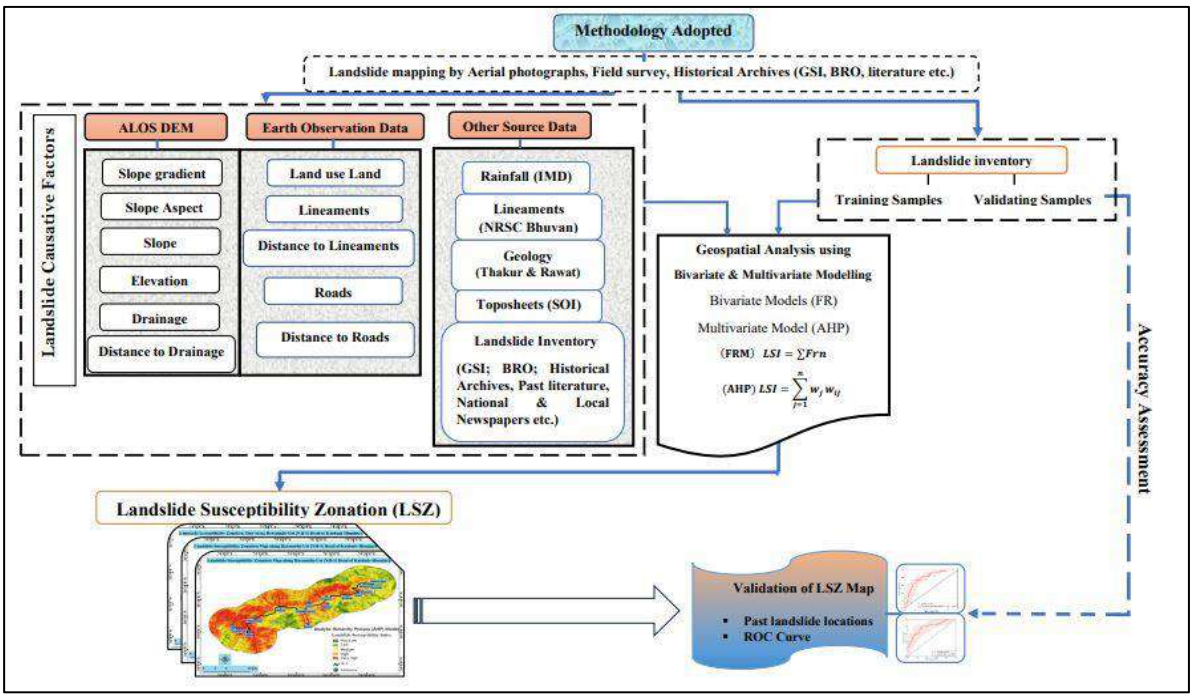

Figure 2 - Flow chart showing different steps of Landslide Susceptibility Zonation (LSZ) adopted in the current study

2.2 Landslide Inventory Mapping

The initial step in establishing a region's vulnerability to landslides is to inspect, detect, and map the landslides (Zhao et al., 2019). The inventory of past landslide locations includes details about current landslides in a region, which helps to validate the map of landslide susceptibility. Field surveys or high-resolution aerial imageries can be used for the purpose. The landslide events were located and mapped for the current study using field inspection and high-resolution images from Sentinel and Google Earth. Generally, spatial mapping of landslides is required to

examine the link between landslide distributions and predisposing factors. Landslide locations were initially located using the GPS coordination system, and then, using high-resolution imagery, the locations of and slides were created as polygons. These historical landslide locations were depicted as point features on the inventory map because they are too tiny to be highlighted at the current scale. The research area has 109 areas where landslides have occurred (Table 1). For model training and validation purposes, the landslide inventory data were split into two groups: training samples (70%) and tested samples (30%). Rockfalls and debris slides were found to be prominent types of landslides along the study road (Fig.3).

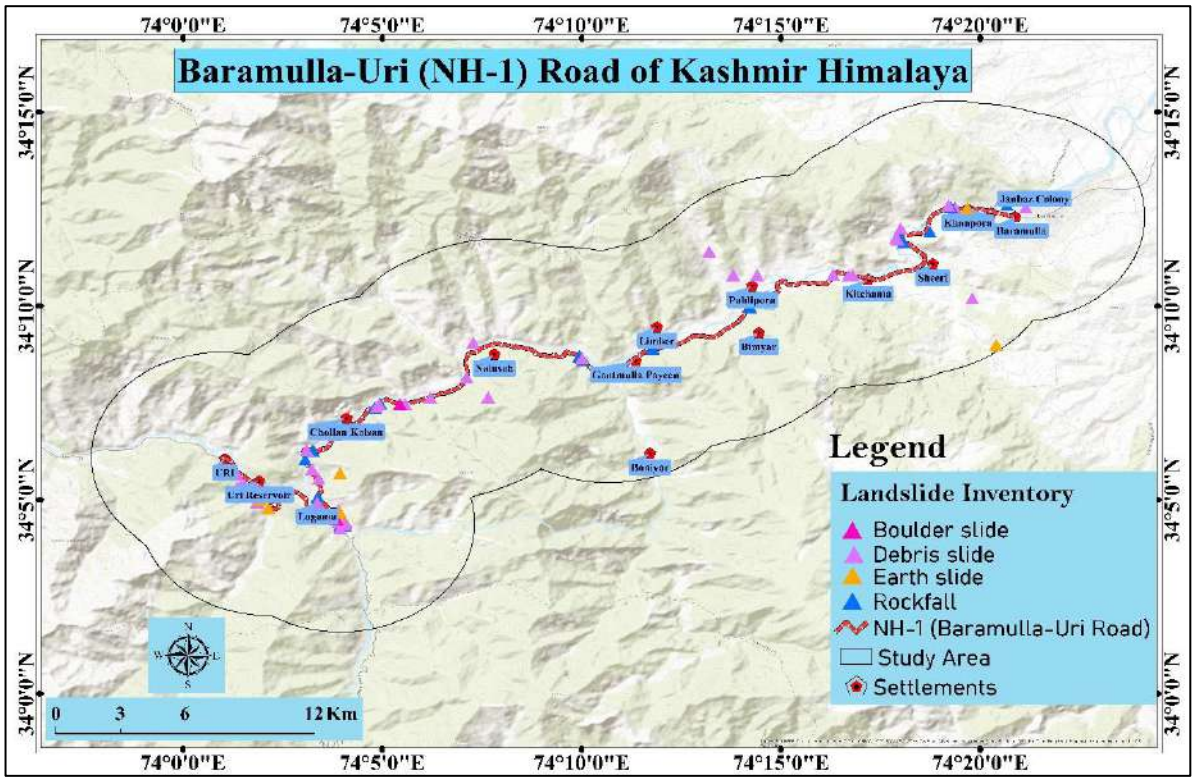

Figure 3 - Landslide Inventory showing different type of landslides, classified based on type of movement in the study area

Table 1 - Showing different types of landslides in the study area

Type of landslide	No. of landslides	Percentage (%)
Rock Fall	35	32.11
Debris Slide	59	54.13
Earth Slide	12	11.01
Boulder slide	3	2.75
Total	109	100

2.3 Landslide Causative Factors

To evaluate landslide Susceptibility, it is crucial to determine what factors contribute to their occurrence. Surface topography limits landslides' density and spatial extent by determining the flow sources and runoff direction (Sujatha et al., 2012).

Topographic factors such as slope gradient, slope aspect, slope curvature, elevation, and natural drainage were retrieved from the Digital Elevation Model (DEM) data at a resolution of 12.5m using the Spatial Analyst tool in ArcMap10.5 (Fig.4a-d). The slope gradient map with a slope ranging from 0° to 80.27° was reclassified into seven distinct classes by applying the Jenks natural breaks classification scheme (Jenk, 1967) (Fig. 4a) viz; 5º (Gentle Slope), 5-8.5º (Moderate Slope), 8.5-16.5º (Strong Slope), 16.5-24º (Very Strong Slope), 24-35º (Extreme Slope), 35-45º (Steep Slope), and >45º (Very Steep Slope). The slope aspect map which represents the direction of slope was reclassified into eight directional classes viz; Northwest (292.5-337.5º), West (247.5-292.5º), Southwest (202.5-247.5º), South (157.5-202.5º), Southeast (112.5-157.5º), East (67.5-112º), Northeast (22.5-67.5º), and North (22.5-337.5º) and one flat (-1) class (Fig. 4b). Most of the current study's landslide areas are along slopes to the north, northwest, and West. The combo curvature (combination of both plane and profile curvature) map was prepared and reclassified the positive values indicated a convex shape, negative values indicated a concave shape, and zero indicated a flat shape (Fig. 4c). Most of the study area constitutes convex class followed by flat and concave classes. In this study, the elevation varies from 1098 to 3475m, reclassified into five classes following Jenk's natural breaks area classification (Fig. 4d). The geological units of the study area include Salkhala Formation, Upper Triassic Limestones, Panjal Volcanics, Thrust, Murree/Dharamshala, Pampur member (Karewa formation), Alluvium, Basement Inliers (Permian-Triassic), Dilpur Formation (Karewa formation), and Hirpur Formation (Karewa formation) was prepared from the Geological map of Jammu and Kashmir (Fig. 4i). Landslides are influenced by alluvium and highly fractured limestone deposits because of their substantial capacity to absorb water. Due to their weak water adsorption capacity and semi-permeability, gneiss and slate-schist are geological rocks that are somewhat prone to landslides.

The land use and land cover features Settlement (Mixed built-up), Barren land, Agriculture, Dense Forest, Scrub/Shrub, Sparse Forest, Pastures, and Waterbodies (Fig. 4h) were visually interpreted by high-resolution satellite imageries, followed by ground truthing. The study region is characterized by extreme rainfall on the southwest mountain slope, while the east slope receives milder rainfall. To obtain an average annual long-period rainfall for the last 30 years, gridded rainfall data from Indian Metrological Data (IMD)was used (NetCDF, 2023). Point data from the gridded data was created and interpolated using Inverse Distance Weighted (IDW) interpolation technique, and the average annual rainfall is found to range from 1014 to 1193mm (Fig. 4j). The study area is reclassified into three categories based on the average annual rainfall: low (1,014 -1,093mm), moderate (1,093 -1,144mm), and high (>1,144mm). The drainage, lineament, and roads were mapped out from the high-resolution satellite imageries and supported by the Survey of India (SOI) toposheets, NRSC Bhuvan web portal, and extensive field survey.

Moreover, the proximity to drainage (Fig. 4e), lineaments (Fig. 4f), and roads (Fig. 4g) were calculated using the Euclidean distance method in ArcGIS 10.5 and reclassified into five classes based on Jenks natural breaks classification. The drainage networks in mountainous regions drastically trigger slope instability and hence make slopes exposed to landslides. Besides the lineament distance has played a significant role in the initiation of landslides. The likelihood of a landslide is thought to be highest in the areas bordering these weak planes and to decrease further from them. Furthermore, the distance from roads is one of the most significant anthropogenic factors influencing the frequency of landslides. Moreover, most of the landslides were found to be localized at the least proximity to intense drainage, lineaments, and along the roads in the study region.

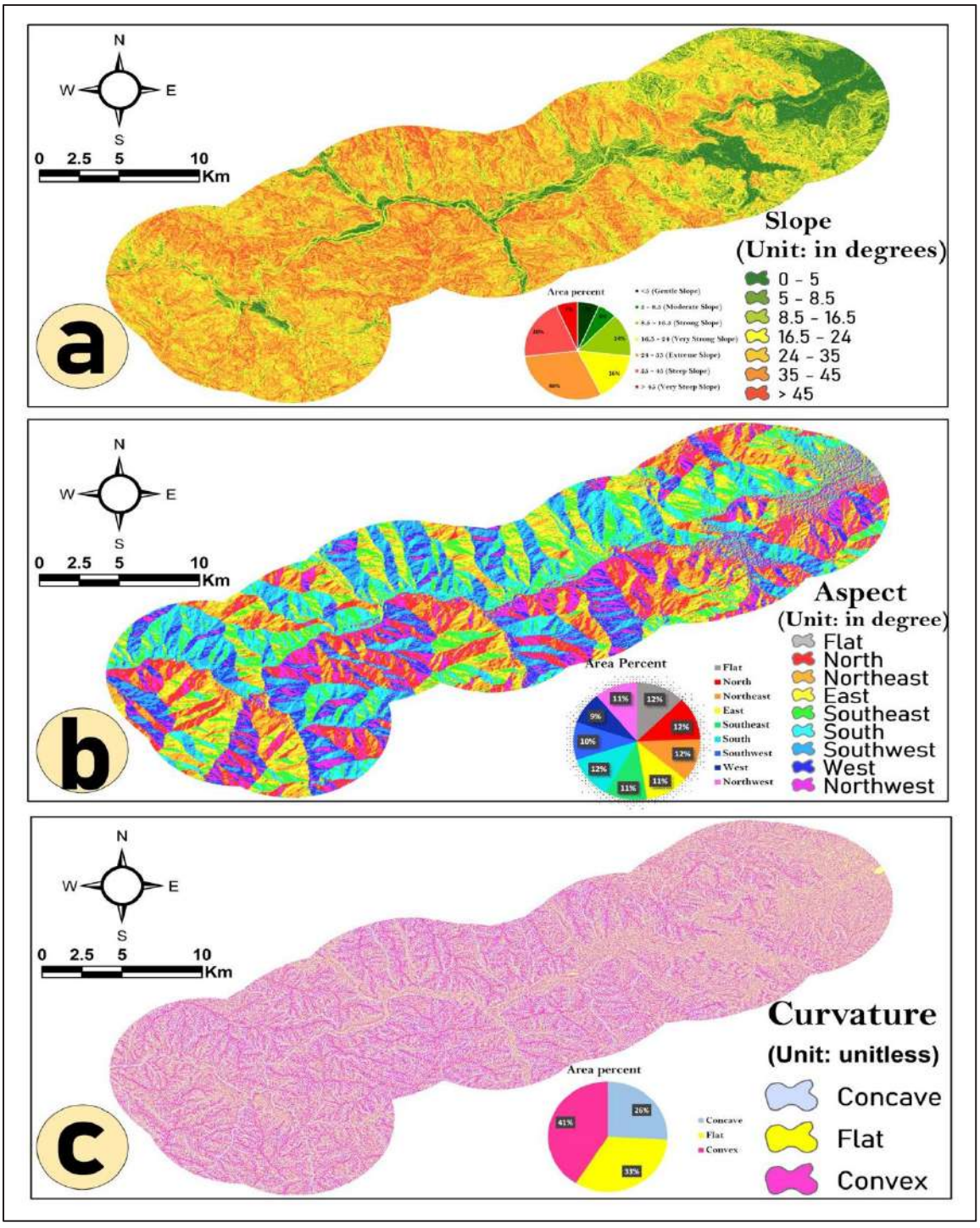

Figure 4 - Landslide causative parameters: (a**)** **S**lope gradient, (b**)** Slope aspect, (c) Slope curvature

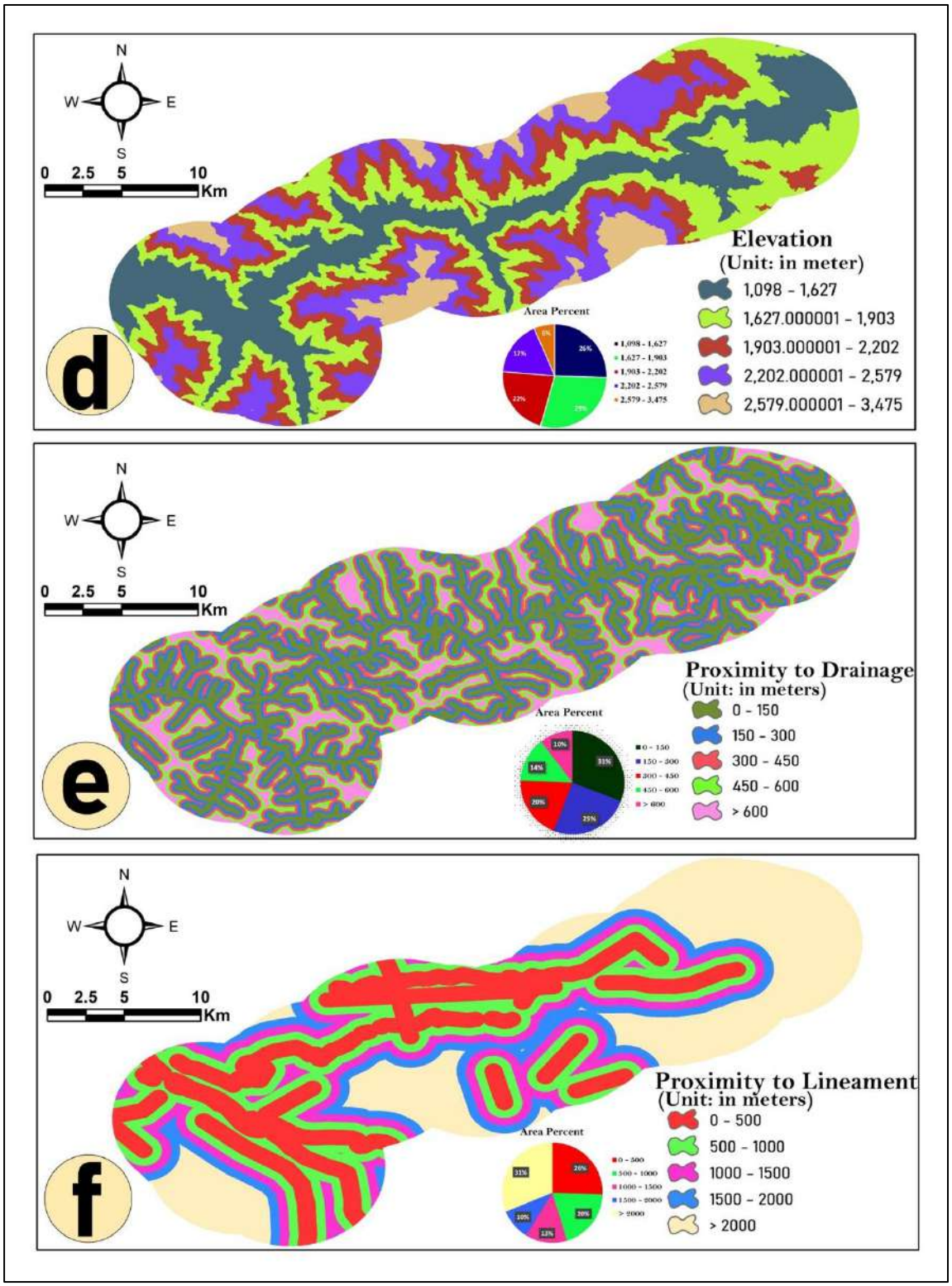

Figure 4 (Contd…) - Landslide causative parameters: (d) Elevation, (e) Proximity to drainage, (f) Proximity to lineaments

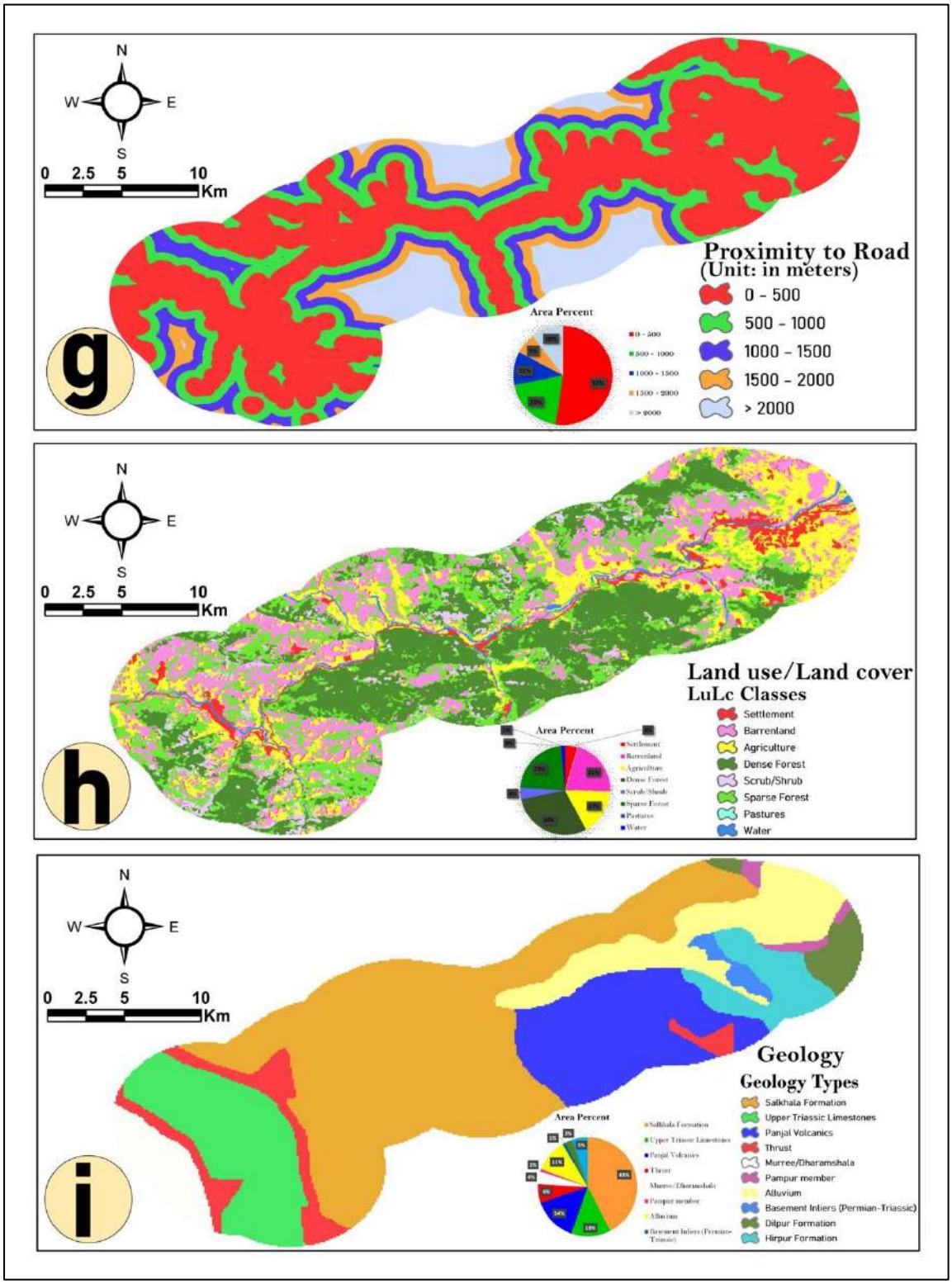

Figure 4 (Contd…) - Landslide causative parameters: (g) Proximity to roads, (h) Landuse/Landcover classes, (i) Geology

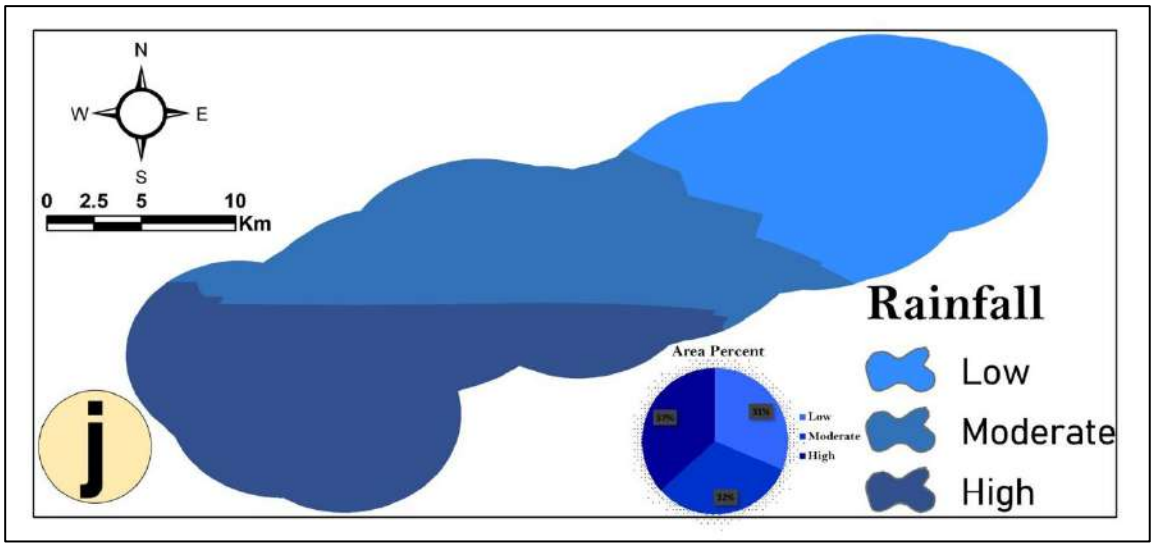

Figure 4 (Contd…) - Landslide Causative parameters: (j) Rainfall

2.4 Methods Adopted

2.4.1 Frequency ratio (FR) model

The frequency ratio method relies on the correlations between the distribution of observed landslides and each factor that controls them. The connection indicates the location of landslide occurrence and the research area's effect elements. The relationship between each class and prior landslide episodes was utilized to compute the frequency ratio of each class in a thematic layer. In the analysis of the relationship between the total area and the region where landslides occurred, a value of 1 represents the mean value. A higher correlation is indicated by a number larger than 1 and a lower correlation is indicated by a value less than 1.

In this analysis, we classify each potential influence into its appropriate category and determine the frequency ratio between categories within the same factor (Eq.1). Normalized frequency ratios are determined for each grouping within the same factor (Eq.2). To determine the landslide hazard index (LHI) (Eq.3), we add up the normalized frequency ratios of the most crucial factors (Pradhan and Lee, 2010; Wang et al., 2016).

Fr_i (Frequency ratio values of class i):

$$Fr_i = \frac{\left(\frac{NL_i}{NL_t}\right)}{\left(\frac{NC_i}{NC_t}\right)} \quad (1)$$

Fr_n (Normalized frequency Ratio values):

$$Fr_n = \frac{Fr_i}{\sum Class\ i Fr} \quad (2)$$

LSI (Landslide susceptibility index):

$$\text{LSI} = \sum Fr_n \tag{3}$$

where NL_i = landslide counts in class i, NL_t = total landslide counts, NC_i = cell point counts of class i and NC_t = total cell points count.

2.4.2 Analytical hierarchy process (AHP) model

The current study uses the Analytical Hierarchy Process (AHP) to classify the potential hazard of landslides in the area. AHP is a semi-quantitative technique for making decisions based on weighted pair-wise relative comparisons (Saaty, 1977). The AHP method is used to calculate the weights associated with the map layer's appropriateness or attribute information (Saaty, 1977). Calculating a list of the relative weights or priority vectors of the components, which can then be coupled with the attribute map layers for hazard zonation, is the next phase of this process (Malczewski, 2004). The weights can be determined by calculating the priority vector of a square reciprocal matrix containing pairwise criteria comparisons. Additionally, the weights must add up to one. Later, Priority Vector weights are mixed with attribute map layers (Malczewski, 2004). Integration of all weighted layers is the subsequent crucial phase in AHP. All AHP computations were performed in a spreadsheet setting. Then, relative weights were utilized in GIS software to overlay layers. AHP solves complicated decision-making problems by constructing a hierarchy of options and factors. Using pair-wise comparison, factors and alternatives are given weights on a nine-point scale. Factors or their classes are grouped in a matrix table with an equal number of rows and columns, with totals listed on one side of the matrix and values of 1 located in the diagonal of the factor matrix (Saaty, 1977; Gorsevski et al., 2006). The pair-wise comparison matrix was constructed in accordance with Saaty (2000) (Table 2).

In this study, the CR value is determined by dividing the values of the indexes CI [consistency index, whose expression is shown in Eq.4)] by the random index RI (Eq.5) (Table 3), which is the average consistency index. Saaty and Vargas (1980) produced the random index table in 1980 based on several random samples (Table 3). A CR of less than 0.1 is acceptable.

$$\text{CI} = \frac{\lambda \max - n}{n-1} \tag{4}$$

where CI = consistency Index value, n = number of criteria utilized for the study (10 in this study), and λmax is the maximum eigenvalue of the comparison matrix.

$$CR = \frac{CI}{RI} \tag{5}$$

where CI is Consistency index value and RI is random index.

The landslide susceptibility index (LSI) using Eq.6 (Thanh and De Smedt, 2012).

$$\text{LSI} = \sum_{j=1}^{n} \left(W_j w_{ij}\right) \tag{6}$$

Where LSI denotes landslide susceptibility index, *Wj* is the weight value of causative factor j, w_{ij} is the weight value of class-I in causative factor *j*, and *n* is the number of causative factors.

Table 2 - AHP preference scale for the comparison of two parameters (Saaty, 2000)

Scales	Strength of preference	Description
1	Equal importance	Two activities contribute equally to the objective
3	Moderate dominance of one over another	Experience and judgments have a slight to moderate tendency toward one activity over another
5	Strong or essential dominance	Experience and judgments strongly or essentially favor one activity over another
7	Very strong or show dominance	An activity is strongly favoured over another, and its dominance is shown in practice
9	Extremely high dominance	The evidence favouring one action over another is extremely strong
2,4,6,8	Intermediate values	Used to designate compromise points between references in weights 1, 3, 5,7, and 9

Table 3 - Number of criteria (N) and random inconsistency (RI) for AHP pairwise comparison (Saaty 2000)

N	2	3	4	5	6	7	8	9	10	11	12	13	14	15
RI	0	0.52	0.9	1.12	1.24	1.32	1.41	1.45	1.49	1.51	1.53	1.56	1.57	1.59

3. RESULTS AND DISCUSSION

The frequency ratio (FR) values were computed using Eq.3. These values were normalized for all the classes present in entire parameter maps based on the relationship with the past landslide locations. Furthermore, the AHP model analysis was carried out through a pairwise comparison of causative factors, and classes within the causative factors were made and normalized to get criteria weight. Therefore, the LSI values for AHP were calculated using Eq.6. For the present study the FR and AHP analysis is carried out which reveals the spatial relationship among landslide inventory and casual factors as shown in Table 4.

Table 4 - FR and AHP model values of for various landslide casual factors

Causative Factors / Classes	Landslide (%)	No. of Pixel in domain	Area (%)	FR_n	AHP		
					w_{ij}	W_j	$W_j w_{ij}$
Slope (degree)				**CR = 0.073**			
<5 (Gentle Slope)	0.00	141943	6.66	0.00	0.022	0.257	0.006
5 - 8.5 (Moderate Slope)	1.59	122522	5.75	0.11	0.033		0.008
8.5 - 16.5 (Strong Slope)	4.76	305461	14.32	0.14	0.058		0.015
16.5 - 24 (Very Strong Slope)	14.29	339445	15.92	0.37	0.096		0.025
24 - 35 (Extreme Slope)	38.10	650933	30.52	0.51	0.155		0.040
35 - 45 (Steep Slope)	25.40	432717	20.29	0.52	0.263		0.068

> 45 (Very Steep Slope)	15.87	139467	6.54	1.00	0.373		0.096
Curvature				CR = 0.061			
Concave (-ive)	31.75	552269	25.90	0.77	0.189	0.033	
Flat (0)	26.98	706399	33.13	0.65	0.081		
Convex (+ive)	41.27	873820	40.98	1.00	0.730		
Aspect				**CR = 0.044**			
Flat (-1)	11.11	266772	12.51	0.38	0.019	0.025	0.000
North (22.5-337.5)	15.87	254885	11.95	0.57	0.024		0.001
Northeast (22.5-67.5)	3.17	251373	11.79	0.11	0.039		0.001
East (67.5-112.5)	0.00	238264	11.17	0.00	0.041		0.001
Southeast (112.5-157.5)	0.00	225927	10.59	0.00	0.051		0.001
South (157.5-202.5)	12.70	253182	11.87	0.46	0.238		0.006
Southwest (202.5-247.5)	15.87	222268	10.42	0.65	0.046		0.001
West (247.5-292.5)	20.63	187482	8.79	1.00	0.214		0.005
Northwest (292.5-337.5)	20.63	232335	10.90	0.81	0.327		0.008
Elevation (m)				**CR = 0.041**			
1,098 - 1,627	98.41	543674	25.49	1.00	0.065	0.044	0.003
1,627.000001 - 1,903	1.59	616741	28.92	0.01	0.132		0.006
1,903.000001 - 2,202	0.00	467180	21.91	0.00	0.291		0.013
2,202.000001 - 2,579	0.00	366416	17.18	0.00	0.479		0.021
2,579.000001 - 3,475	0.00	138477	6.49	0.00	0.065		0.003
Proximity To Drainage (m)				**CR = 0.041**			
0 - 150	76.19	656874	30.80	1.00	0.034	0.115	0.004
150 - 300	19.05	535585	25.12	0.31	0.068		0.008
300 - 450	3.17	419016	19.65	0.07	0.134		0.015
450 - 600	1.59	298438	13.99	0.05	0.295		0.034
> 600	0	222575	10.44	0.00	0.470		0.054
Proximity To Lineament (m)				**CR = 0.042**			
0 500	49.21	544560	25.54	1.00	0.035	0.206	0.007
500 - 1000	7.94	421674	19.77	0.21	0.075		0.015
1000 - 1500	22.22	286690	13.44	0.86	0.137		0.028
1500 - 2000	15.87	214499	10.06	0.82	0.289		0.060
> 2000	4.76	665065	31.19	0.08	0.464		0.096
Proximity To Roads (m)				CR = 0.034			
Rainfall (mm)				**CR = 0.061**			
Low	17.46	669312	31.39	0.34	0.081	0.061	0.005
Moderate	22.22	680214	31.90	0.42	0.189		0.012
High	60.32	782962	36.72	1.00	0.730		0.045

Geology				**CR = 0.013**			
Salkhala Formation	28.57	905106	42.44	0.21	0.025	0.084	0.002
Upper Triassic Limestones	41.27	275104	12.90	1.00	0.206		0.017
Panjal Volcanics	7.94	306468	14.37	0.17	0.061		0.005
Thrust	6.35	130159	6.10	0.33	0.033		0.003
Murree/Dharamshala	0.00	88144	4.13	0.00	0.044		0.004
Pampur member	0.00	19176	0.90	0.00	0.084		0.007
Alluvium	11.11	226987	10.64	0.33	0.257		0.022
Basement Inliers (Permian-Triassic)	1.59	23022	1.08	0.46	0.020		0.002
Dilpur Formation	0.00	51548	2.42	0.00	0.156		0.013
Hirpur Formation	3.17	106774	5.01	0.20	0.115		0.010
Landuse/Landcover				**CR = 0.01**			
Settlement (Mixed buit-up)	74.60	94239	4.42	1.00	0.025	0.02	0.001
Barren	11.11	449909	21.10	0.03	0.206		0.004
Agriculture	3.17	355100	16.65	0.01	0.061		0.001
Dense Forest	4.76	631871	29.63	0.01	0.033		0.001
Scrub/Shrub	0.00	89370	4.19	0.00	0.044		0.001
Sparse Forest	3.17	481447	22.58	0.01	0.084		0.002
Pastures	0.00	262	0.01	0.00	0.257		0.005
Water	3.17	30290	1.42	0.13	0.020		0.000

3.1 Landslide Susceptibility Zonation

Landslide susceptibility analysis has been carried out through bivariate and multivariate methods. In the current study, the frequency ratio, and analytical hierarchy process models were adopted. For the application of frequency ratio, relative effect, and analytical hierarchy process models, all ten landslide causative factors were converted to a raster format with 15x15 m size grids to calculate the landslide susceptibility index (LSI). All the causative factors were taken to the spatial analysis extension of the ArcGIS software for integration. The LSI was calculated based on the integration rules as shown in Eqs. 3 and 6. The integration was carried out using the raster calculator option of the ArcGIS software. If the LSI value is high, it means a higher susceptibility to landslides; a lower value means a lower susceptibility to landslides. For the frequency ratio model, the minimum, mean, maximum, and stanard deviation of LSI are 1.25999999, 4.590958959, 10, and 1.507434622, respectively. While in the case of analytical hierarchy process, the LSI values had a minimum value of 1, a mean value of 5.623002599 and a maximum value of 9, with a standard deviation of 1.105878348.

Furthermore, the LSZ maps prepared using FR, RE and AHP methods were classified into five susceptibility classes viz., very low, low, moderate, high, and very high based on Jenks natural breaks classification method (Fig. 5a, b). In FR model 22 % of the training landslide areas were identified in high and very high susceptibility classes and in case of AHP model, 54 % of the training landslide areas were identified in the high and very high susceptibility classes (Fig.6).

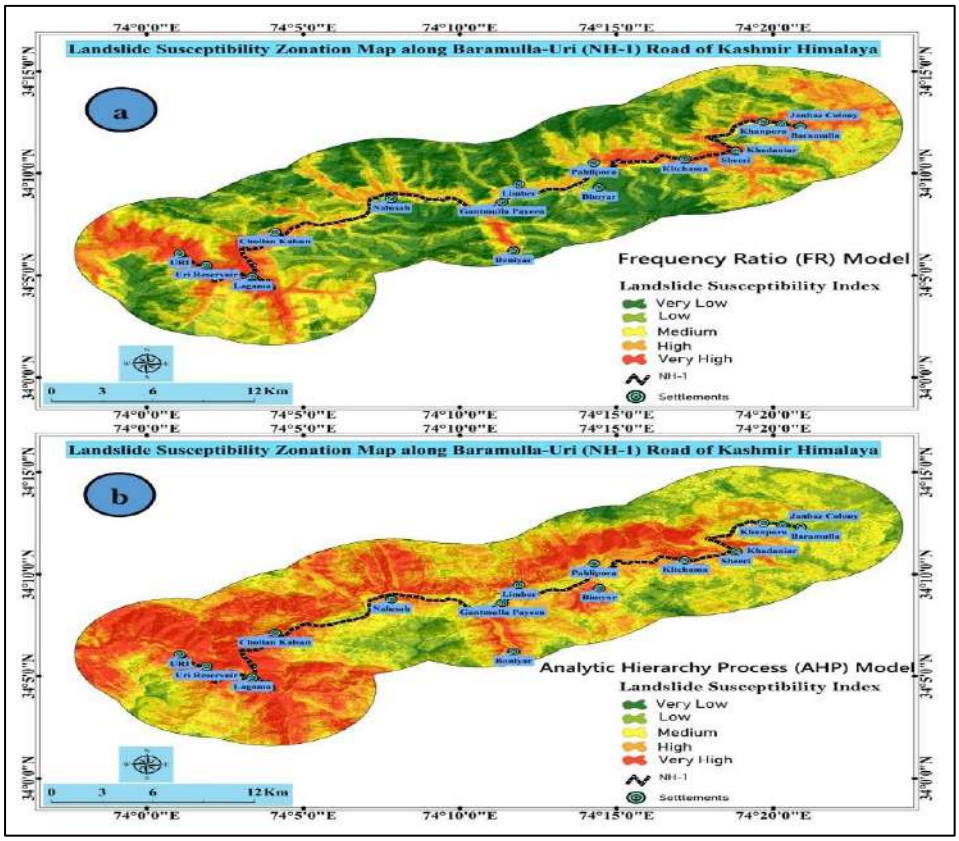

Figure 5 - LSZ maps (**a)** Frequency ratio model, **(b)** Analytical hierarchy process

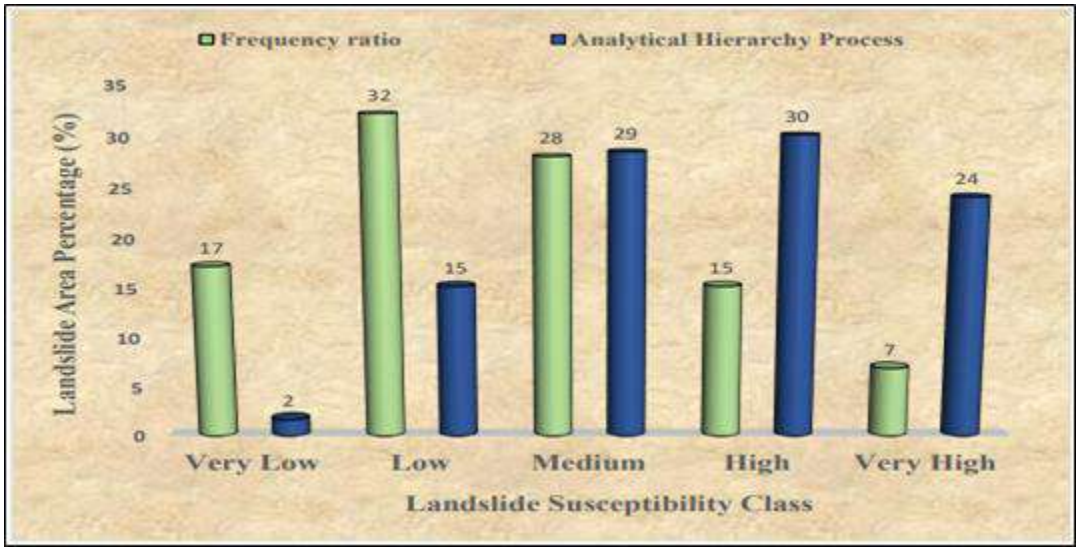

Figure 6 - Landslide area percentage and susceptibility class for FR and AHP LSZ maps

3.2 Comparison and Validation of the Models

In the present study, the most common Receiver operating characteristic (ROC) method was adopted to determine the prediction accuracy (prediction rate) of each model. ROC curves have been widely employed in susceptibility map evaluation (Mallick et al., 2018).

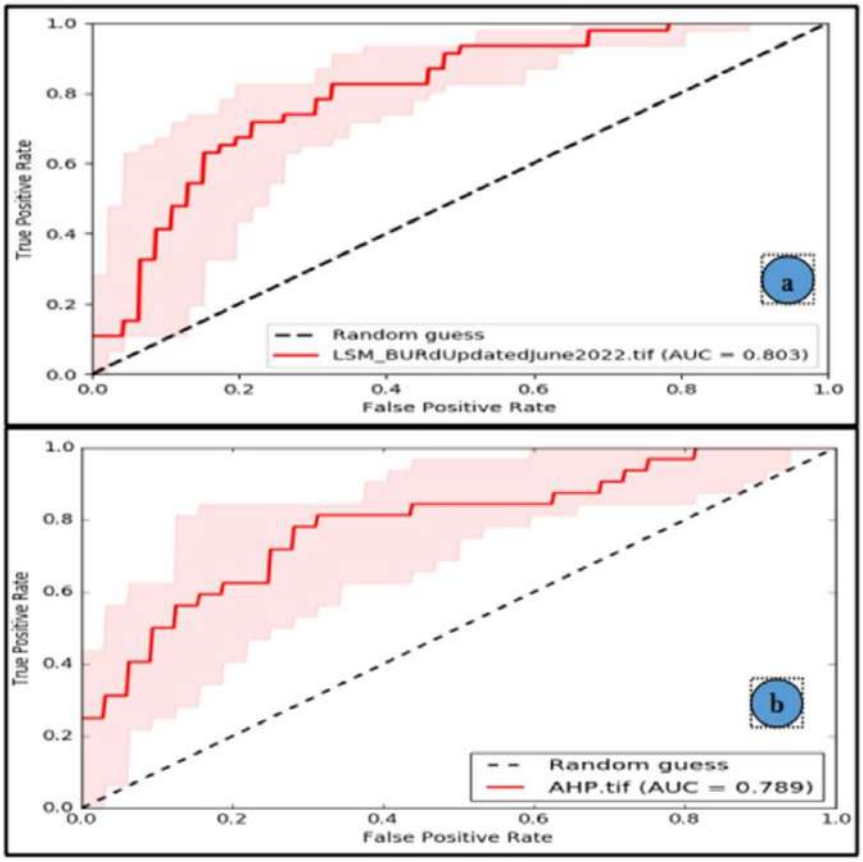

Figure 7 - ROC Curve of (a) FR and (b) AHP models

The Area under curve (AUC) value of ROC was determined through the integration of validation landslide dataset with LSZ maps. If the AUC value close to 1.0 indicates the model is ideal, whereas an AUC value close to 0.5 reflects the in accuracy in the model (Fawcett, 2006). The AUC Value of prediction rate curve (Fig. 7a, b) for FR and AHP models was found to be 0.803 and 0.789. A detailed field investigation was conducted in the research area (Fig.8).

The validation result indicates that the resultant susceptibility maps and existing landslide location datasets are in good agreement. During validation, a high level of good agreement was found between the LSZ maps and pre-existing landslide location datasets. Therefore, it suggests that almost all landslide locations fall under the high and very high susceptibility categories. While comparing all the models with each other based on AUC values, the map produced by the FR model presented the best result for landslide susceptibility evaluation. As a result, the FR model was found to be a reliable and effective method for estimating landslide-susceptible areas. However, the map's reliability depends on the data collection's precision, the method's robustness, and the landslide prediction experience.

4. LIMITATIONS OF THE STUDY

It is imperative to acknowledge the limitations of the study. Ten causal elements were considered in the study. However, additional variables, including rock properties, soil properties, and seismic activity, were not considered. Furthermore, the study did not account for the temporal variability of the causative factors, which can impact the landslide hazard zones. In addition, secondary data sources were utilized, which may have introduced some

constraints regarding precision and spatial resolution. Moreover, Subjectivity is a major drawback of AHP. The expert's assessment greatly affects results. However, this research shows that the AHP's technique performs better when field circumstances and attributes are appropriately determined by experts. The frequency ratio (FR) is easy to use, gives accurate results, and can show how much each type of causal factor affects the occurrence of a landslide. However, the FR method doesn't look at how causal factors affect each other. In some ways, the integrated method could maintain the advantages of the FR and AHP methods while limiting their drawbacks. This makes the predictions more accurate and gives a more viable map that can be used for landslide hazard management.

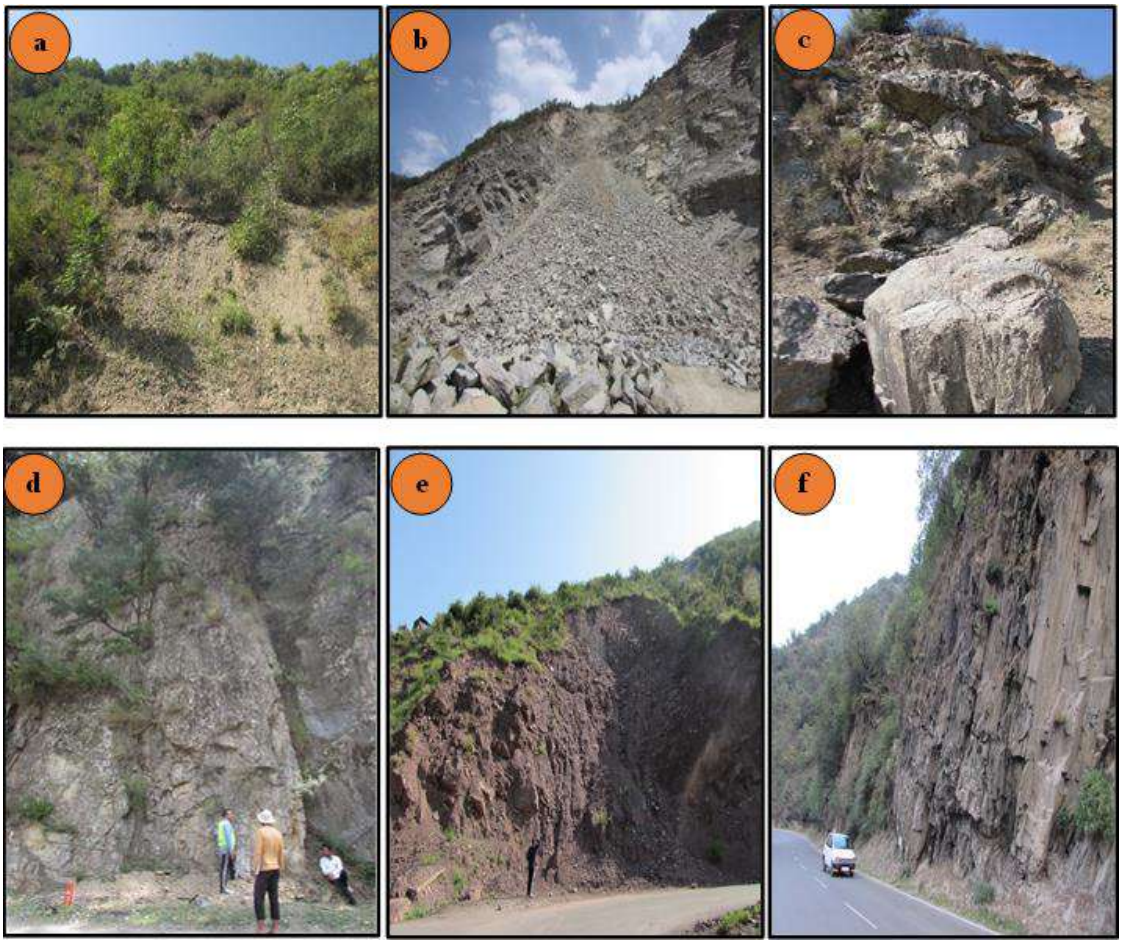

Figure 8 - Field photographs of few recent landslides in the study region (a) Earth slide near Lagama (b) Debris flow near Khanpora (c) Boulder slide main mohra +1.5 km (d) Rockfall near Gantamulla Debris flow near Lagama (f) Rockfall near Bonyar park along Baramulla-Uri (NH-1) roadside

5. CONCLUSIONS

In the present study, frequency ratio, and analytical hierarchy process were adopted for the landslide susceptibility mapping along a part of NH-1, Kashmir Himalaya. Landslide susceptibility maps have been produced using the relationship between each land slide-influencing parameter and known landslide locations. The results have shown that the occurrence of landslides was more predominant along cut slope, slope gradient >24°, convex curvature, and elevation in 1098-1627 m categories, geology type (upper Triassic limestone),

settlement (mixed built-up), west, Northwest, south, proximity to drainage(0-150m), proximity to lineaments (0-500m), and proximity to roads within the distance of 0-500 m classes. The validation results show that the frequency ratio model has better prediction accuracy (AUC = 0.803) than the relative effect model (AUC = 0.761), and analytical hierarchy process (0.789).

The overall study results show that the areas such as Limber, Chollan Kalsan, Uri, Sheeeri, Baramulla, Boniyar, Janbazcolony, Khanpora, Kichama, Lagama, and Khadaniar were identified as highly vulnerable to landslide occurrences. Anthropogenic interferences in this hilly terrain have caused a huge impact on the slopes and the condition is worsened as the internal properties of the lithology and the overlying debris material are weak due to which slope instability is triggered. The landslide susceptibility maps are the source for decision-making and developmental activities in an area. Moreover, the output results of the present study could help the developers, planners, and engineers for slope management and land-use planning in the study area.

Acknowledgements

The authors thank the Border Roads Organization (BRO) Srinagar, J&K, India, and the Geological Survey of India (GSI) for providing necessary landslide data. In addition, the authors would like to express their gratitude to everyone who assisted in the present study. Finally, the authors also thank anonymous reviewers for their valuable comments and suggestions.

References

Fawcett T. (2006). An introduction to ROC analysis, Pattern recognition letters, 27(8):861-874.

Fell R., Corominas J., Bonnard C., Cascini L., Leroi E., Savage W.Z. (2008). Guidelines for landslide susceptibility, hazard, and risk zoning for land use planning, on behalf of the JTC-1 joint technical committee on Landslides and engineered slopes, Eng. Geol., 102:85–98.

Gorsevski P.V., Jankowski P. and Gessler P.E. (2006). A heuristic approach for mapping landslide hazard by integrating fuzzy logic with analytic hierarchy process, Control. Cyber, 35:21-141.

Guzzetti F., Carrara A., Cardinali M., Reichenbach P. (1999). Landslide hazard evaluation: a review of current techniques and their application in a multi-scale study, Central Italy, Geomorphology, 31:181-216.

Malczewski J. (2004). GIS-based land-use suitability analysis: a critical overview, Prog Plan, 62:3-65.

Mallick J., Singh R.K., Al Awadh M.A., Islam S., Khan R.A., Qureshi M.N. (2018). GIS-based landslide susceptibility evaluation using fuzzy-AHP multi-criteria decision-making techniques in the Abha Watershed, Saudi Arabia, Environmental Earth Sciences, 77:1-25.

NetCDF (2023). Yearly grided rainfall data. Data pertaining to the last 30 years. IMD Pune, Retrieved from: https://www.imdpune.gov.in/cmpg/Griddata/Rainfall_25_NetCDF.html.

Pradhan B. and Lee, S. (2010). Landslide susceptibility assessment and factor effect analysis: backpropagation artificial neural networks and their comparison with frequency ratio and bivariate logistic regression modelling, Environ. Modell. Softw., 25(6):747-759. https://doi.org/10.1016/j.envsoft. 2009.10.016.

Saaty T.L. (1977). A scaling method for priorities in hierarchical structures, J. Math Psychol, 15:231-281.

Saaty T.L. (2000). Fundamentals of Decision Making and Priority Theory, 2nd ed., RWS Publications.

Saaty T.L., Vargas L.G. (1980). Hierarchical analysis of behavior in competition: prediction in chess, Behav. Sci., Vol.25, No.3, pp. 180–191. https://doi.org/10.1002/ bs.3830250303.

Sujatha E.R., Rajamanickam G.V., Kumaravel P. (2012). Landslide susceptibility analysis using probabilistic certainty factor approach: a case study on Tevankarai stream watershed, India, J. Earth Syst Sci., 121(5):1337-1350.

Thakur V.C., Jayangondaperumal R., Malik M.A. (2010). Redefining Medlicott–Wadia's main boundary fault from Jhelum to Yamuna: an active fault strand of the main boundary thrust in northwest Himalaya, Tectonophysics, 489:29-42. http://dx.doi.org/10.1016/j.

Thanh L.N., De Smedt F. (2012). Application of an analytical hierarchical process approach for landslide susceptibility mapping in A Luoi district, Thua Thien Hue Province, Vietnam, Environ Earth Sci., 66(7):1739-1752.

Varnes D., IAEG. (1984). Landslide hazard zonation: a review of principles and practice, U N Sci Cult Organ, Paris, pp. 1-6.

Wang Q., Li W., Yan S., Wu Y., Pei Y. (2016). GIS based frequency ratio and index of entropy models to landslide susceptibility mapping (Daguan, China), Environ. Earth Sci., 75(9): 1-16. https://doi. org/10.1007/s12665-016-5580-y.

Zhao Y., Wang R., Jiang Y., Liu H., Wei Z. (2019). GIS-based logistic regression for rainfall-induced landslide susceptibility mapping under different grid sizes in Yueqing South-eastern China, Eng Geol., 259:105147.